Published in final edited form as:
J Cell Sci. 2008 April 1; 121(Pt 7): 1128–1137. doi:10.1242/jcs.016865.

Analysis of protein domains and Rett syndrome mutations indicate that multiple regions influence chromatin-binding dynamics of the chromatin-associated protein MECP2 in vivo

Asmita Kumar[1], **Sachin Kamboj**[2], **Barbara M. Malone**[1], **Shinichi Kudo**[3], **Jeffery L. Twiss**[1,4], **Kirk J. Czymmek**[4], **Janine M. LaSalle**[5], and **N. Carolyn Schanen**[1,4,*]

1 *Nemours Biomedical Research, Alfred I duPont Hospital for Children, Wilmington, DE 19803, USA*

2 *Department of Computer and Information Sciences, University of Delaware, Newark, DE 19716, USA*

3 *Department of Biological Science, Hokkaido Institute of Public Health, N-19 W-12, Kita-ku, Sapporo 060-0819, Japan*

4 *Department of Biological Sciences, University of Delaware, Newark, DE 19716, USA*

5 *Department of Medical Microbiology and Immunology, University of California, Davis, CA 95616, USA*

Summary

The methyl-CpG-binding protein 2 (MECP2) serves both organizational and transcriptional functions in the nucleus, with two well-characterized domains integrally related to these functions. The recognition of methylated CpG dinucleotides is accomplished by the methyl-binding domain (MBD), and the transcriptional repression domain (TRD) facilitates protein-protein interactions with chromatin remodeling proteins. For each known function of MECP2, chromatin binding is a crucial activity. Here, we apply photobleaching strategies within the nucleus using domain-deleted MECP2 proteins as well as naturally occurring point mutations identified in individuals with the neurodevelopmental disorder Rett syndrome (RTT). These studies reveal that MECP2 is transiently associated with chromatin in vivo and confirm a central role for the MBD in directing the protein to heterochromatin. In addition, we report for the first time that the small region between the MBD and the TRD, known as the interdomain region (ID), stabilizes chromatin binding by MECP2 independently of the MBD. The TRD of MECP2 also contributes towards chromatin binding, whereas the N- and C-termini do not. Some common RTT missense and nonsense mutations significantly affect binding kinetics, suggesting that alterations in chromatin binding can result in protein dysfunction and hence a disease phenotype.

Keywords

Methyl-binding domain; Methylation; Inter domain region; Photobleaching; Epigenetics

Introduction

Methylation of cytosine residues in CpG dinucleotides is a major epigenetic modification that modulates chromatin-mediated transcriptional repression and silencing (reviewed by Wade, 2001). Proteins possessing the methyl-binding domain (MBD) specifically bind to methylated CpG nucleotides and form complexes with other chromatin modifiers to generate changes in

*Author for correspondence (e-mail: schanen@medsci.udel.edu).

regional chromatin structure that affect transcriptional activity and/or genome stability. The prototypical member of the MBD family is the methyl-CpG-binding protein 2 (MECP2) (Nan et al., 1993), a multifunctional protein that is best known as a transcriptional repressor that interacts with chromatin remodeling complexes containing histone deacetylases (HDAC) (Jones et al., 1998; Nan et al., 1998). Supporting this role, MECP2 has been co-immunoprecipitated with Sin3a and HDAC1/2 (Jones et al., 1998; Nan et al., 1998; Suzuki et al., 2003), as well as the silencing mediator for retinoid and thyroid hormone receptors (SMRT) (Stancheva et al., 2003) and the histone methyltransferase, Suv39H (Fuks et al., 2003). Interaction with the Sin3a and HDAC1/2-containing complexes occurs via a region designated as the transcriptional repression domain (TRD) (Nan et al., 1997). Notably, MECP2 does not completely co-fractionate with these partners, suggesting that it is not a component of a stably assembled complex (Klose and Bird, 2004).

MECP2 binds to both unmodified DNA as well as to methyl CpG dinucleotides, with increased affinity for symmetrically methylated DNA; thus, it is typically distributed throughout the nucleus and enriched in DAPI-bright heterochromatic regions in interphase murine nuclei (Koch and Stratling, 2004). In differentiating murine myocytes, MECP2 participates in the assembly of pericentromeric heterochromatin, and exogenous overexpression of MECP2 leads to aggregation of chromodomains in perinucleolar foci in a dose-dependent manner (Brero et al., 2005; Marchi et al., 2007). Differences in chromosome structure and nuclear organization between murine and human cells are evidenced by distinct patterns of MECP2 localization in human cells. For example, in MCF breast cancer cell (MCF-7), MECP2 is distributed throughout the nucleus and appears granular. It also does not completely correlate with CpG methylation and heterochromatic regions, and is excluded from classic satellite DNA in the interphase nucleus (Koch and Stratling, 2004).

Functionally, the prevailing model for MECP2 holds that it stably associates with chromatin, facilitating both long-range and short-range transcriptional repression through chromatin remodeling and assembly of chromatin loops (Horike et al., 2005; Yasui et al., 2007). MECP2 has also been shown to bind specific gene targets to regulate transcription directly. This interaction can be modulated through phosphorylation, indicating that the interactions may not be static and can be influenced by extracellular stimuli (Chen et al., 2003; Martinowich et al., 2003; Zhou et al., 2006; Miyake and Nagai, 2007). Additionally, Klose et al. reported that the association of MECP2e2 with chromatin is dynamic through photobleaching approaches (Klose et al., 2005). Thus, it appears that MECP2 plays multiple roles in the nucleus, not only acting as a global transcriptional repressor through long-range chromatin remodeling, but also as a contextual modulator of specific gene targets. For each of these activities, the affinity with which MECP2 binds to chromatin is a crucial determinant of its function(s) in vivo.

MECP2 also appears to participate in cellular activities beyond those of an epigenetic transcriptional repressor and at least some of those functions involve domains of the protein outside the MBD and TRD. For example, the C-terminal region of the protein has been implicated in RNA-mediated functions based on co-immunoprecipitation of MECP2 with WW domain splicing factors (Buschdorf and Stratling, 2004) and the RNA-binding factor, YB1 (Young et al., 2005). There are two mammalian isoforms of MECP2, which are identical except for their short unique N-termini (Kriaucionis and Bird, 2004; Mnatzakanian et al., 2004). The more recently identified MECP2e1 (MECP2α/MECP2b) isoform arises through alternative splicing of exon 2 and generates a protein with an acidic N-terminus compared with the MECP2e2 (MECP2β/MECP2a) isoform (theoretical pI for the unique N-terminal regions: MECP2e1=4.25, MECP2e2=9.5). Although the functional distinction for the two protein isoforms is not known, expression of the transcript variants is developmentally and regionally regulated in postnatal mouse brain, with MECP2e1 becoming the predominant form in the mature animal (Dragich et al., 2007).

Mutations in the X-linked *MECP2* gene occur in the neurodevelopmental disorder Rett syndrome (RTT). Examination of the type and location of the disease alleles sheds light on the relative importance of individual protein domains for function. Missense mutations cluster in the MBD, whereas most nonsense mutations lie in the interdomain region (ID) and TRD. Frameshift mutations most often occur in the C-terminal region. Mutations occur infrequently in the N-terminal region of MECP2e1, and to date no mutations have been identified in the unique N-terminus of MECP2e2. Functional assays on a number of RTT mutations interspersed over the length of the gene demonstrate aberrant localization on chromatin or impair transcriptional repression functions of some mutant proteins, other clearly pathological mutations are functionally indistinguishable from wild-type (WT) protein when assessed using in vitro functional assays (Ballestar et al., 2000; Kudo et al., 2003; Yusufzai and Wolffe, 2000). The inability to detect dysfunction probably arises because of multiple factors that can modulate the function of a chromatin-binding protein, including intrinsic (amino acids that are necessary for making crucial DNA-protein or protein-protein contacts) or extrinsic (local chromatin structure) factors, or a combination of both. Given the complex interactions of MECP2 with numerous nuclear proteins, it is crucial to study the dynamics of its chromatin association in the context of intact chromatin in living cells. We therefore employed a systematic mutagenesis approach to study the role of individual protein domains, common missense and nonsense RTT mutations, and DNA methylation towards governing MECP2 kinetics in vivo.

Results

MECP2e1 and MECP2e2 completely colocalize and exhibit indistinguishable and rapid kinetics in the nucleus

The N-termini of the two MECP2 isoforms vary considerably in charge, prompting us to study their localization and chromatin binding kinetics. Stable cell lines expressing murine MECP2e1-EGFP and MECP2e2-EGFP under the heavy metal inducible metallothionein I promoter (MT1) were generated in Balb/c 3T3 fibroblasts. We chose this promoter so that we could exploit its leakiness to obtain basal levels of MECP2 expression that do not perturb chromatin structure. Inspection of uninduced cells indicated that both forms were exclusively nuclear and preferentially associated with DAPI-rich foci, similar to previously reported immunolocalizaton studies in mouse nuclei [Kriaucionis and Bird (Kriaucionis and Bird, 2004); Fig. 1A]. In addition, the salt elution profiles of the endogenous and EGFP-tagged proteins were similar, indicating that the EGFP-tagged MECP2 proteins bound to chromatin with similar avidity to that of the endogenous proteins (supplementary material Fig. S1). Together, these results indicated that tagging MECP2 with EGFP did not alter its localization or its binding affinity for chromatin, and validated the use of tagged constructs for functional studies of MECP2.

Initial experiments revealed that both isoforms of MECP2 associated with DAPI-rich regions, indicative of heterochromatin. We therefore examined the localization of MECP2e1-EGFP and MECP2e2-ECFP in the same cell by confocal microscopy using filter sets that allowed the isolation of the EGFP and ECFP signals individually despite overlapping emission spectra. Owing to the relative weak signal of ECFP compared with EGFP, cells were induced with 100 μM Zn^{2+} to facilitate visualization. These studies revealed that both proteins exhibited identical nuclear and heterochromatin localization patterns, and that they appeared to completely colocalize (Fig. 1B), indicating that the proteins were targeted to the same regions of the nucleus and suggesting a degree of functional redundancy. MECP2e2-EGFP colocalized with other heterochromatin marker proteins, including heterochromatin protein 1 (HP1) and histone H3 trimethylated at lysine 9, clearly indicating its strong preference for association with heterochromatic regions (Fig. 1C). A recent report demonstrated a physical association

between MECP2 and HP1 in vivo during myogenic differentiation (Agarwal et al., 2007). Our localization studies were consistent with previous immunolocalization studies that showed that MECP2e2 was preferentially associated with heterochromatin and exhibited no detectable association with other nuclear regions or cytoplasm (Nan et al., 1996).

We next asked whether similar localization of the two MECP2 isoforms translated into comparable chromatin-binding characteristics. To address this issue, we used fluorescence recovery after photobleaching (FRAP) to study the dynamics of MECP2 binding. In contrast to salt elution approaches, FRAP allows measurements to be made in vivo with resolution at the single-cell level. Hence, we used this approach to examine the mobility of MECP2e1 and MECP2e2 in the pericentromeric heterochromatin foci where the protein was enriched. These analyses revealed that both isoforms were mobile in vivo, and showed indistinguishable and rapid kinetics with overlapping recovery curves (Fig. 2). It took 20.8±5.6 and 21.3±5.4 seconds, respectively, for the bleached MECP2e1-EGFP and MECP2e2-EGFP regions to recover 50% of their pre-bleach intensity (t^{50}). Notably, even within dense constitutive heterochromatin domains, the majority of both forms of MECP2 were mobile, with ~90% recovery of pre-bleach intensity within 200 seconds following the bleach pulse (Table 1). In euchromatic regions, MECP2 displayed extremely rapid recovery kinetics (t^{50}=0.125±0.003 seconds), similar to a soluble protein (Fig. 2D), with essentially full recovery of fluorescence indicating a minimal fraction of immobile protein. These binding kinetics were similar to those recently reported by Marchi et al. For MECP2e2 (Marchi et al., 2007); however, we found a smaller fraction of immobile protein (10% versus 25%), probably reflecting differences in expression of the murine versus the human protein in the murine 3T3 cells (Marchi et al., 2007). Thus, we conclude that both isoforms of MECP2 transiently associate with chromatin in living cells, exhibiting distinct kinetics in heterochromatin and euchromatin.

Mobility of MECP2 in the nucleus is not dependent on methylation status of the DNA

MECP2 has increased affinity for methylated DNA (Meehan et al., 1992; Nikitina et al., 2007) and therefore we asked whether the chromatin-binding characteristics of MECP2e2 were altered by changes in the methylation status of chromatin. DNA demethylation was accomplished by treating Balb/c 3T3 cells with 5 Aza-2-deoxycytidine prior to transfection with expression constructs for photobleaching. Results from these studies showed that there was limited change in MECP2 mobility following DNA demethylation in both pericentromeric heterochromatin and euchromatin. Although a modest leftward shift in the recovery curve was noted following DNA demethylation in heterochromatin, the difference did not reach statistical significance (P=0.0798). The binding characteristics of MECP2 in the euchromatin were indistinguishable in cells treated with or without 5-Aza-2-deoxycytidine (Fig. 3).

Differential localization and kinetics of mutant MECP2 proteins

Using a series of domain deletion mutants derived from the MECP2e2-EGFP construct, we next examined the contribution of the individual domain(s)/region(s) towards chromatin localization and binding (Fig. 4A). Basal expression of each of these constructs in stable cell lines revealed production of EGFP-tagged truncated proteins that ranged from ~60–100 kDa (supplementary material Fig. S3). Notably, by western blot, the ΔMBD construct consistently showed significantly higher expression than the other constructs. While this may reflect an increase in efficiency in extraction of the ΔMBD protein, the variability of expression among cells within a transfected pool, as well as potential differences in expression between individual constructs, necessitated use of strict nuclear fluorescence criteria to select nuclei for FRAP assays to control for expression effects.

Localization of the domain-deleted proteins was examined using fluorescence microscopy to detect the EGFP-labeled MECP2 proteins in DAPI-stained nuclei. The deletion of the N-

terminus (ΔN), interdomain region (ΔID) and the C-terminus (ΔC) had no impact on the enrichment of the mutant proteins in heterochromatin (Fig. 4B). These results indicate that these domains or regions were not responsible for heterochromatin targeting of the protein. By contrast, the MBD-deleted protein (ΔMBD) was visibly mislocalized, and was excluded from heterochromatic foci (Fig. 4B). Notably, the mutant protein was not diffusely localized in the nucleus but was found to accumulate in nucleoli, as revealed by immunostaining with the nucleolar marker protein nucleolin (Fig. 4C), a nuclear domain from which it is normally completely excluded (see WT in Fig. 4C). The functional significance of this nucleolar accumulation was unclear; however, no evidence for a dominant-negative effect was detected; the heterochromatic regions appeared grossly normal (Fig. 4C, DAPI staining for WT versus ΔMBD) and micrococcal nuclease treatment of the mutant cell lines were similar to WT (supplementary material Fig. S2). The TRD deletion mutant (ΔTRD) exhibited both nuclear and cytoplasmic localization (Fig. 4B,D). Incomplete nuclear entry for this mutant protein was expected because of the loss of the primary NLS, which lies within the TRD. Nuclear accumulation of a fraction of the ΔTRD deletion mutant argues that there are one or more additional functional NLS(s) in other regions of the protein. Sequence analyses predict a potential second NLS between residues 174 and 190 in the ID region of MECP2 (http://psort.nibb.ac.jp). It is notable that the protein that was imported into the nucleus showed the characteristic heterochromatin localization of the WT protein.

We measured the kinetics of chromatin association of the domain-deleted proteins compared with full-length/WT proteins to isolate the contribution of the individual domains to the chromatin-binding properties of the protein. Deletion of either the N- or the C-terminal regions led to a slight leftward shift in the early recovery curve. However, the kinetics were not significantly different from the WT protein (Fig. 5), indicating that these regions did not make major contributions to the overall chromatin-binding properties of MECP2. By contrast, deletion of the MBD disrupted the chromatin-binding properties of MECP2e2-EGFP dramatically (Fig. 6). As the protein was localized in the nucleus and was enriched in nucleoli, we performed photobleaching in nucleoplasmic regions outside these nucleolar territories. The relative t^{50} of the MBD deletion mutant in the nucleoplasm was 1.3±0.4 seconds compared with 0.125±0.003 seconds in euchromatin for the WT protein (Fig. 5B). This increase in the t^{50} of the MBD-deleted protein probably arose from a mixture of heterochromatin and euchromatin within the nucleoplasmic region selected for photobleaching (as we could not use the MECP2-EGFP signal as a surrogate marker for heterochromatin). The kinetics of this mutant resembled the kinetics of the high mobility group (HMG) proteins that have a t^{50} of about three seconds (Phair and Misteli, 2000) and approached that of freely diffusible EGFP (data not shown).

Unexpectedly, deletion of the ID region (residues 163–206) also resulted in markedly accelerated binding kinetics with a t^{50} of 5.3±2.1 seconds (Fig. 6B). This protein appeared properly localized, so it was unlikely that deletion of the ID disrupted folding of the MBD, and this suggested that this region was important for stabilizing MBD-dependent interactions. Similarly a RTT truncation mutation in the interdomain region R168X also localized to heterochromatin, but exhibited very rapid kinetics (t^{50}=1.17±0.5 seconds) (Fig. 7). The R168X mutant was found in both the cytoplasm and the nucleus, suggesting that there was yet another unidentified NLS within the first 168 residues of MECP2 (supplementary material Fig. S4). Thus, the presence of a MBD did not confer stable binding in the absence of the ID region residues. The MBD, however, was necessary and sufficient for targeting the protein to heterochromatin.

Deletion of the TRD also had a significant effect on protein mobility within the heterochromatic nuclear foci (t^{50}=7.9±2.5 seconds), consistent with data indicating that the TRD contributes to DNA/chromatin binding and facilitates protein-protein interactions between MECP2 and other

proteins, and that these interactions slow the release of MECP2 from chromatin (Adams et al., 2007; Nan et al., 1998). Two AT-hooks were predicted between residues 185–197 (in the ID region) and residues 265–277 (in the TRD) (http://elm.eu.org/). However, mutagenesis of crucial arginine residues to aspartic acid in these AT-hooks (R190D and/or R270D) had no discernible effect on localization of binding kinetics (data not shown), similar to previous studies (Klose et al., 2005).

Common RTT mutations exhibit impaired binding kinetics

The domain deletion studies were used to gain a global insight into the regions of the protein that are necessary for chromatin binding by MECP2, but such large internal deletions are seldom found in the patient population. As such, we investigated the impact of common RTT missense and nonsense mutations on MECP2 binding to chromatin. The effects of these mutations on DNA binding, nuclear localization and transcriptional repression have been previously reported (Kudo et al., 2001; Kudo et al., 2003; Nikitina et al., 2007). For these studies, the EGFP-MECP2e2 expression constructs were transiently transfected into Balb/c 3T3 cells. Despite the species difference and relative overexpression compared with the murine constructs used in the domain deletion studies, the kinetics for the WT protein were not significantly different, although there was an increase in the immobile fraction with the human constructs (Figs 2 and 7). Interestingly, a truncation mutation in the TRD (R255X) had no impact on the mobility of MECP2, suggesting that residues 254–486 were dispensable for proper MECP2 binding to chromatin (Fig. 8), consistent with recent studies by Marchi et al. (Marchi et al., 2007). This result lends support to the observation that deletion of the C-terminus did not impact the dynamics of MECP2 (Fig. 5).

We also examined the binding kinetics for four common recurrent missense mutations in the MBD of human MECP2. The mutants chosen have been previously investigated using in vitro approaches, and had inconsistent results in terms of their ability to bind to methylated DNA, to localize to heterochromatin or to repress reporter transcription (Ballestar et al., 2000; Yusufzai and Wolffe, 2000; Kudo et al., 2003). R106W, R133C and F155S were reported to show substantially impaired in vitro binding to methylated DNA, while T158M exhibited only a twofold decrease (Ballestar et al., 2000; Yusufzai and Wolffe, 2000). Similar to previous reports and the MECP2e2-EGFP data, mutations in the MBD led to mislocalization of the protein for most of these alleles, with only the R133C protein enriched in the heterochromatic foci (data not shown) (Kudo et al., 2003). The binding properties of each of the mutations tested, R106W, R133C, F155S and T158M, differed from the kinetics of WT protein. R106W, T158M and F155S exhibited very rapid kinetics (t^{50} of 1.4±0.42, 1.5±0.5 and 1.4±0.3 seconds, respectively), whereas R133C exhibited intermediate kinetics (t^{50} of 12.4±4.5 seconds) between WT and the other mutants. These results revealed that each of the mutants tested were defective in chromatin binding in vivo, which could result in impaired function of the protein.

In summary, we have carried out a systematic analysis of chromatin dynamics of MECP2 with a goal of identifying key residues and regions of the protein that facilitate in chromatin binding by MECP2 in vivo. Our results support previous reports that have identified the MBD as a major DNA and chromatin-binding domain. Additionally, we report that the ID region is crucial for proper chromatin association of MECP2, and that this appears to be independent of the function of the putative AT hook located in this region of the protein. The TRD, which has recently been shown to bind DNA (Adams et al., 2007), also contributes to chromatin binding of MECP2 in the nucleus.

Discussion

Using photobleaching strategies, we directly measured the kinetic properties of the association of MECP2 with chromatin in vivo and examined the stability of these interactions. Our studies

demonstrate that even within highly condensed and heavily methylated constitutive heterochromatin domains, the majority of the population of MECP2 is, at best, only transiently associated with chromatin. In non-heterochromatic regions, the recovery profile of MECP2 approaches soluble proteins. These results are in agreement with previous biochemical studies, which demonstrated that the entire population of MECP2 could be extracted with 0.5 M NaCl (Meehan et al., 1992). Notably, the linker histone, H1, which displays similar salt extraction and mobility profiles, is also dynamically associated with chromatin (Lever et al., 2000; Misteli et al., 2000). Similarly, heterochromatin protein 1 (HP1) associates transiently with chromatin in vivo, and all HP1 isoforms recover completely following photobleaching in heterochromatic regions with a t^{50} between 2.5 and 50 seconds in different cell lines (Cheutin et al., 2003; Festenstein et al., 2003). By contrast, the core histones are virtually statically associated with chromatin (Kimura and Cook, 2001), with over 50% of the population of histone H2B and ~80% of the total population of histone H3 and H4 appearing immobile using FRAP approaches. Thus, chromatin-protein mobility does not directly correlate with transcriptional activity or chromatin state, as, even within highly compacted regions of the genome, many of the associated proteins bind evanescently, and long-term chromatin association of transcriptional modulators is not necessary for stable repression of chromatin-mediated functions.

To examine the contribution that the individual domains/regions of MECP2 make towards protein chromatin binding, we systematically deleted or mutated the known domains/regions and examined localization and binding properties of the protein. These studies clearly indicate that the MBD performs a central role in the enrichment of MECP2 in heterochromatic regions of the nucleus, and in establishing the primary binding properties of the protein. Complete deletion of the domain generated a protein that mislocalized to the nucleolus and displayed kinetics comparable with a soluble protein. Further dissection of this domain was accomplished using a group of pathogenic RTT mutations and suggested that the methyl-CpG-binding function of the MBD only partially contributes to the binding kinetics. This is supported by the observation that the R133C mutation, which alters one of the five residues that make the hydrophobic methyl-binding pocket (Free et al., 2001; Wakefield et al., 1999), had the least impact on mobility of the four alleles tested. Previous analyses of this mutation have yielded somewhat conflicting results in terms of its effect on DNA binding (Free et al., 2001; Nan et al., 2007; Yusufzai and Wolffe, 2000). However, our data lend support to the premise that the R133C allele is truly hypomorphic, consistent with data indicating that it retains the ability to bind methylated DNA (Nan et al., 2007) and repress transcription in vitro (Kudo et al., 2003), and that individuals with the R133C allele tend to be more mildly affected (Leonard et al., 2003). By contrast, mutation of residues R106 and F155, which lie away from the DNA-protein interface and are thought to be important for protein folding and structure of the MBD (Heitmann et al., 2003; Ohki et al., 1999; Wakefield et al., 1999), led to proteins that were indistinguishable from the MBD-deleted protein in these assays in that they were similarly mislocalized and highly mobile in the nucleoplasm. Mutation of these residues has previously been shown to disrupt folding of the MBD (Free et al., 2001). Notably, a recent study by Marchi et al. (Marchi et al., 2007) found that introduction of the R106W mutation disrupted binding of a truncated form of MECP2 containing only the N-terminal and MBD segments of the protein (Marchi et al., 2007). The solution structure of the MBD of MECP2 reveals that T158 lies towards the C-terminus of the domain away from the DNA interface (Ohki et al., 2001). Thus, mutation of this residue has been predicted to minimally perturb the DNA-binding functions of the protein (Free et al., 2001). This was supported by in vitro binding assays that demonstrated that the avidity for methylated DNA of the T158M mutant decreased by a mere twofold compared with over 100-fold reduction in the case of the R106W, R133C and F155S alleles (Ballestar et al., 2000; Free et al., 2001). However, in other studies, residual function of the T158M protein was more significantly impaired (Kudo et al., 2001; Yusufzai and Wolffe, 2000). In the present study, this mutation clearly had a significant impact on the mobility of

the protein within the nucleoplasm, suggesting that this residue is important for proper interaction of MECP2 with chromatin in the context of a living nucleus. Although the basis for this is not known, given the position of this residue within the MBD, it is possible that the mutation disrupts the folding of the MBD and/or adjacent ID regions.

In addition to the MBD, we also found that other regions/domains of the protein appear to strengthen the association of MECP2 with chromatin, most probably through charge-based protein-DNA and protein-protein interactions facilitated by its highly basic amino acid composition, as approximately one-fifth of all residues in MECP2 are basic. Two regions identified in these studies as important contributors to chromatin binding in vivo were the ID and TRD. The ID-deleted protein was enriched in heterochromatin, but displayed accelerated kinetics, suggesting that the entire region, or a part of the region, contributes towards chromatin binding. This increase in mobility did not reflect direct loss of MBD function as the ID deletion did not impinge upon residues in the MBD. The ID is a short region made up of 44 amino acids, of which about 30% of the residues are basic, and has a theoretical pI of 12.02. It is a highly disordered part of the protein and has a similar amino acid composition to the HMGA1 protein (Adams et al., 2007). One could surmise that the high density of basic residues in this region may play a role in stabilizing MECP2 binding by facilitating the association of the phosphate backbone of DNA with this charged domain. Of note, the ID was included in the region that was mapped as the site of interaction of MECP2 with co-repressors (Nan et al., 1998) and, in *Xenopus*, is the region that associates with p20, a putative protease inhibitor that stabilizes MECP2 (Carro et al., 2004). Thus, it is possible that the stabilization of the chromatin binding imparted by the ID region is also conferred by protein-protein interactions. Notably, although the region includes a potential AT-hook motif, our data indicate that this module does not appear to influence mobility because mutation of the key arginine residue (R190D) had no effect on binding kinetics. The R168X RTT mutation, which truncates the protein in the ID region, exhibited rapid kinetics, similar to those observed in the ID deletion mutant. This result was predicted based on our domain deletion data but argue against the model presented by Stancheva et al., who suggested that this truncated form could not interact with co-repressors leading to a failure of this mutant to release appropriately from chromatin (Stancheva et al., 2003).

Deletion of the TRD also altered the kinetics of heterochromatin binding by MECP2, though not to the same extent as the MBD or ID deletions. This may result from compromised ability to bind to chromatin directly or because deletion of the TRD abolishes the interaction of other protein(s) that stabilize the association of MECP2 with chromatin, or a combination of the two. Recent data indicate that the TRD alone shows non-specific DNA binding in vitro (Adams et al., 2007); however, whether this is the case in vivo is not known. Notably, the binding kinetics for the R255X RTT mutant protein and the C-terminal deletion mutant were comparable with the WT protein, allowing us to refine the region involved in stabilization of the interaction to residues 256–309. Taken together, our data clearly indicate that proper binding requires function of the MBD, ID and TRD working in conjunction with each other.

Mutations in the C-terminal of MECP2 occur in ~20% of individuals with RTT, who are often less severely affected (Smeets et al., 2005). An intriguing observation about this region is that it shows the highest incidence of frameshift mutations compared with any other region of MECP2 (Shahbazian and Zoghbi, 2001). To further lend support to the involvement of this region in RTT pathogenesis, a mutant mouse lacking the C-terminus (truncation at R308) exhibits RTT-like phenotype, suggesting that this region of the protein is important for MECP2 function (Shahbazian and Zoghbi, 2002). Surprisingly, deletion of the C-terminus of MECP2 was not found to impact the avidity of association of MECP2 with chromatin in Balb/c 3T3 cells or NIH 3T3 cells (Marchi et al., 2007) even though the C-terminus has been implicated in the methylation independent general DNA binding of MECP2 to both naked DNA and to

nucleosomes reconstituted in vitro (Chandler et al., 1999). In addition, Georgel et al. have demonstrated that MECP2 can condense DNA and nucleosomal arrays to form higher order chromatin structure independent of DNA methylation and other proteins in vitro. This group has also shown that this chromatin condensing property of MECP2 resides in the region that is not translated in the RTT truncation mutation R168X (Georgel et al., 2003).

The function of the N-terminus of the protein remains enigmatic, although the two protein isoforms vary only in this region. Localization and binding kinetics were essentially identical for the N-terminal deleted protein and both protein isoforms, consistent with redundancy in their function, despite the sequence differences at the N-terminus. Given that MECP2e1 is the major isoform (~10 fold higher that MECP2e2) expressed in the brain (Dragich et al., 2007; Mnatzakanian et al., 2004), this suggests that it may have an important neuronal role that may have eluded detection in our fibroblast-based assays. It is plausible that the domains/regions identified as not being necessary for chromatin binding of MECP2 may play a role towards aiding in other functions of MECP2 once the protein is bound to chromatin. It should be stressed that photobleaching experiments are limited to the resolution of extrinsic and intrinsic changes, which impact binding characteristics.

These deletion studies allowed identification of regions within MECP2 that are important for its association with chromatin. It should be noted that the size of the deletion had no correlation on its impact on binding. The C-terminus deletion was the largest domain removed, and had no distinguishable impact on chromatin association relative to WT protein. However, deletion of the smallest 44 amino acid ID region had a significant impact on chromatin binding as did point mutations within the MBD or ID. Although our studies with these deletion mutants provide important information about their contribution to overall chromatin binding, we cannot exclude position effects or improper folding of an adjacent domain.

The multiple protein domains in MECP2 allow it to modulate numerous functions independently and in concert with each other. Among its many reported functions, the best-characterized roles of MECP2 are as an architectural nuclear protein, and as a transcriptional repressor (Chadwick and Wade, 2007), two activities that are not necessarily mutually exclusive. As such, traditional models for MECP2 function hold that it partakes in long-term and stable repression of transcription of methylated DNA via interfacing with chromatin remodeling proteins that generate repressive structures. However, in recent years, a contextual role for the involvement of MECP2 in gene-specific expression has emerged. Microarray-based studies of gene expression using brain tissue failed to identify global changes in gene expression in MECP2 mutant mice compared with their WT counterparts (Tudor et al., 2002), leading a number of investigators to apply candidate gene strategies to identify MECP2 targets. As a result, a number of genes that are subject to MECP2-based repression have been identified, and the list is growing rapidly (Chen et al., 2003; Drewell et al., 2002; Horike et al., 2005; Martinowich et al., 2003). It is thought that MECP2 scans for methylated CpG nucleotides, binds and associates with co-repressors, including Sin3a, which then recruits HDAC1/2 to form a complex that catalyzes the formation of repressive chromatin structure, impeding the movement of the transcriptional machinery (Jones et al., 1998; Nan et al., 1997; Nan et al., 1998). Whether MECP2 functions as a ‘global’ or ‘gene-specific’ repressor, chromatin binding is required for it to perform its function.

The rapid binding kinetics of MECP2 in combination with its relatively promiscuous association with other nuclear proteins as detected by co-immunoprecipitation assays (Fuks et al., 2003; Harikrishnan et al., 2005; Kimura and Shiota, 2003; Kokura et al., 2001; Suzuki et al., 2003) suggests that transient association of MECP2 with chromatin may be sufficient for it to attract chromatin-remodeling proteins to methylated DNA. However, once the complex is initiated, MECP2 is no longer required to continue the process and can dissociate, leaving

the binding site vacant and available to be bound by competing proteins. Throughout the nucleus, MECP2 binding is in flux, the protein potentially volleying between binding to chromatin and local binding partners. In constitutive heterochromatin, the enrichment of potential interacting proteins has a stabilizing effect, albeit a transient one, on its binding kinetics. In these regions, MECP2 may serve a largely structural role by organizing chromatin domains, which indirectly and directly modulate gene expression. However, in euchromatic regions, the protein binds fleetingly to chromatin, where it may play a more pivotal role in regulating specific gene targets.

Materials and Methods

Plasmids

The coding regions of mouse *Mecp2e2* and *Mecp2e1* were amplified from IMAGE clones 4948925 and 6515311 (American Type Culture Collection, Manassas, VA) using the following PCR primers: *Mecp2e1*, forward 5′-GGCCGGCCATGGCC-GCCGCTGCCGC-3′; *Mecp2* reverse 5′-CGCGGCCGCGCTAACTCTCTCGGTC-3′; and *Mecp2e2* forward 5′-GGCCGGCCATGGTAGCTGGGATGTT-3′and *Mecp2* reverse. ΔN was amplified with ΔN forward 5′-GGCCGGCCCATGTCGGCT-TCCCCCA-3′and *Mecp2* reverse. ΔMBD was generated by fusing two PCR products (ΔMBD_N and ΔMBD_C) together. ΔMBD_N was amplified with forward 5′-GGCCGGCCATGGTAGCTGGGATGTT-3′ and reverse 5′-GCTAGCGGCTTC-TGGCACTGCTGGG-3′. ΔMBD_C was generated by PCR amplification with forward 5′-GCTAGCGGGAGCCCCTCCAGGAGAG-3′ and *Mecp2* reverse. ΔID was generated by fusing two PCR products (ΔID_N and ΔID_C). ΔID_N was generated with forward 5′-GGCCGGCCATGGTAGCTGGGATGTT-3′ and reverse 5′-GCTAGCCCTCTCCCAGTTAC-3′. ΔID_C was generated by forward 5′-GGCTAGCGCAGGTGAAAAGG-3′ and *Mecp2* reverse. ΔTRD was made by fusing two PCR fragments (ΔTRD_N and ΔTRD_C) together. ΔTRD_N was amplified with forward 5′-GGCCGGCCATGGTAGCTGGGATGTT-3′ and reverse 5′-GCTAGCACACCTTCTGATGC-3′. ΔTRD_C was amplified with forward 5′-GCTAGCGACGGTCAGCATCG-3′ and *Mecp2* reverse. ΔC was made with forward primer 5′-GGCCGGCCATGGTAGCTGGGATGTT-3′ and reverse 5′-GCGGC-CGCCTCCCGGGTCTTGCGCT-3′.

The amplified products were fused in frame with EGFP, EYFP and ECFP amplified from pEGFP-N3, pEYFP-N1 and pECFP-N1 (Clontech, Mountain View, CA) using primer sets: EGFP forward 5′-GCGGCCGCGATGGTGAGCAAGGGCG-3′ and EGFP reverse 5′-AGCGCTTTACTTGTACAGCTCGTCC-3′. The fused product was inserted into the MTH1^{0}Aneo vector from which the coding region of H1^0 had been excised. The fusion constructs were placed under the control of the MT1 promoter. All plasmids were confirmed by sequencing.

The generation of RTT mutant constructs, which encode human MECP2e2 with an N-terminal EGFP under control of the CMV promoter, have been previously described (Kudo et al., 2001). R168X was generated by site-directed mutagenesis using the full-length human MECP2e2 construct as the template for mutagenesis.

Generation and propagation of stable cell lines and transfection

Stable cell lines were generated in Balb/c 3T3 mouse fibroblast cells. All transfections were carried out with the Lipofectamine 2000 reagent (Invitrogen, Carlsbad, CA) according to the manufacturer's instructions. Stably transfected cells were selected and maintained in 400 μg/ml G418. All experiments were conducted on uninduced cells expressing basal levels of fusion proteins. Cell lines chosen for experiments exhibited similar levels of basal expression based

on the relative amount of EGFP-tagged protein compared with endogenous protein in the same number of cells.

Immunofluorescence

Stable cell lines expressing EGFP-tagged MECP2 constructs were grown on poly-L-lysine coated coverslips and fixed with 4% paraformaldehyde in phosphate-buffered saline (PBS) for 10 minutes. Coverslips were washed with PBS for 5 minutes, and then treated with methanol for 4 minutes. Cells were washed three times with PBS containing 0.1% Tween (PBST) for 10 minutes and blocked for 30 minutes with 10% normal serum in PBST. The normal serum used for blocking and diluting antibodies was serum from the host animal in which the secondary antibody was raised. Coverslips were incubated in the following primary antibodies diluted in 1% normal serum in PBST for 2–4 hours in a humidifying chamber at 37°C: α-HP1β (1:500; Millipore, Billerica, MA); α-H3 trimethylated at K9 (1:1000; Upstate, Lake Placid, NY) and α-Nucleolin (1:50; Santa Cruz, Santa Cruz, CA). Coverslips were washed three times with PBST for 10 minutes. Secondary antibodies were diluted in 1% normal serum in PBST, and incubations were performed for 1 hour. Coverslips were washed with PBST and mounted with Vectashield containing DAPI (Vector Laboratories, Peterborough, UK) and imaged on a DMRXA2 epifluorescence microscope (Leica Microsystems) equipped with a cooled CCD camera (Hamamatsu ORCA-ER, Hamamatsu-City, Japan) and OpenLab 3.1.3 software (Improvision, Lexington, MA).

Imaging of EGFP- and ECFP-tagged MECP2 isoforms

Images were acquired using a 40× Plan-Neofluar (NA 1.3) oil immersion objective lens on a Zeiss Axiovert 200M microscope equipped with a Zeiss LSM 510 META confocal microscope. All spectral data for multi-labeled samples were collected with simultaneous 458 nm (ECFP, EGFP) excitation using the 30 mW argon laser in online fingerprinting mode. Spectral scans were acquired in a single pass using a 10.7 nm window from 463–548 nm. Reference spectra were acquired from individually labeled fluorescence protein controls and used for online linear unmixing to cleanly separate the overlapping ECFP and EGFP signals.

Photobleaching

FRAP was performed as described previously (Phair and Misteli, 2000) using a Leica TCS-SP2 confocal microscope equipped with an environmental chamber to maintain temperature at 37°C (Life imaging services, Reinach, Switzerland). Cells were cultured on Labtek chambered cover glass system (Nalge Nunc, Rochester, NY). Cells selected for photobleaching had a nuclear intensity of 10–25 arbitrary units. Approximately 5% of the total nuclear area was bleached. The area to be bleached was chosen such that an entire pericentromeric heterochromatin focus could be bleached. In mutants that did not show accumulation of the protein in heterochromatin foci, a nucleoplasmic area representing 5% of the total nuclear area was bleached. Care was taken to avoid perinucleolar and perinuclear regions while selecting the region to photobleach. Five prebleach scans were performed at 323 mseconds at 7% laser power of the 488 laser line. Two bleach pulses of 323 ms each were administered at 100% laser power. One-hundred post-bleach scans were performed at 7% laser power. The intensity of the region of interest was normalized to the pre-bleach intensity as well as the total nuclear fluorescence to generate recovery curves for individual nuclei using the equation $Irel=T^0 X I^t/T^t X I^0$, where T^0 is the mean total intensity and I^0 is the mean regional fluorescence in the prebleach images, and T^t and I^t are the total and regional values at each timepoint, respectively.

Curve fitting to generate t^{50} values and statistics

The t^{50} values were obtained by fitting individual recovery curves to the equation: $f(x)=a + (b - a) \times x / (x + c)$, where f(x)=intensity; x=time; a=intensity immediately after the bleach pulse;

b=maximum intensity and c=t^{50}. The average t^{50} value for each group was calculated from the t^{50} values of individual subjects. Two-tailed, unpaired *t*-tests were performed to compare the t^{50} value of WT against mutants with statistical significance set at $P<0.05$.

Chromatin structure analysis

Nuclei were isolated from cells as previously described (Richard-Foy and Hager, 1987). 2×10^5 nuclei were resuspended in wash buffer supplemented with 250 μM $CaCl_2$ and 1 U micrococcal nuclease [10 mM Tris (pH 7.6), 15 mM NaCl, 60 mM KCl, 0.15 mM spermine and 0.5 mM spermidine]. Digestion was carried out for 10 minutes at room temperature and the reaction was stopped with micrococcal nuclease termination buffer [0.5% SDS, 2 mM EDTA, 1 mM EGTA (pH 7.6)]. Proteins were digested with Proteinase K at 50°C for 12–14 hours. DNA was extracted twice with phenol chloroform, ethanol precipitated and resolved on a 1.8% Metaphor agarose gel (Cambrex, East Rutherford, NJ) and visualized by ethidium bromide staining.

Salt elution of MECP2

Nuclei were isolated as described above and resuspended in wash buffer [10 mM Tris (pH 7.6), 15 mM NaCl, 60 mM KCl, 0.15 mM spermine and 0.5 mM spermidine]. An equal volume of salt extraction buffer [100 mM Tris (pH 7.6), 0–1000 mM NaCl, 1% protease inhibitor cocktail (Sigma, St Louis, MO)] and resuspended nuclei were mixed by rotation for 1 hour at 4°C. The slurry was centrifuged at 21,100 ***g*** for 15 minutes, and the supernatant was collected. The pellet was extracted stepwise with salt solution [100 mM Tris (pH 7.6) containing 1 M NaCl] to isolate the population of MECP2 that was still bound to chromatin. Proteins were resolved on a 7.5% SDS/PAGE, and analyzed by immunoblotting with an antibody directed towards a C-terminal epitope of MECP2 (Thatcher et al., 2005). The resultant blots were quantified using Image J software (http://rsb.info.nih.gov/ij/).

For quantitation of amount of EGFP-tagged proteins compared with endogenous MECP2 levels, whole-cell lysates were prepared in homogenization buffer. Nuclear proteins were extracted with 1M NaCl, precipitated with TCA and processed for SDS/PAGE and immunoblotting.

Western blotting of cell lines expressing EGFP-tagged-domain-deleted proteins

Whole-cell extracts were prepared by homogenizing cells in homogenization buffer supplemented with 500 mM NaCl and protease inhibitor cocktail. The crude extract was rotated on a rotating platform for 1 hour at 4°C and centrifuged at 18,400 ***g*** for 15 minutes at 4°C. The supernatant was collected, resolved on a 4–15% gradient SDS-PAGE and processed for immunoblotting.

5-Azadeoxycytidine treatment of cells

1×10^4 Balb c/3T3 cells were seeded and allowed to attach for 24 hours in two-well Labtek chambered cover glasses. Cells were treated with 1 μM 5-azadeoxycytidine or DMSO (vehicle) for 5 days before transfecting them with the human MECP2e2-EGFP construct driven by the CMV promoter. Photobleaching was performed 24–48 hours after transfection.

Supplementary Material

Refer to Web version on PubMed Central for supplementary material.

Acknowledgements

The authors thank David T. Brown (University of Mississippi Medical Center) for his generous gift of the MTH1^{0}Aneo vector, Guoping Fan (University of California, Los Angeles) for his gift of the IAP plasmid, and Dhananjay Yellajoshyula for helpful suggestions and discussions. This research was supported by the Abigail Brodsky Award from International Rett Syndrome Association (IRSA) to A.K. and by NIH/NICHD R01-HD37874 to N.C.S. Core services were provided through the Nemours Center for Pediatric Research Biomedical Core Laboratory supported by NIH P20-RR020173 and the Nemours Foundation.

References

Adams VH, McBryant SJ, Wade PA, Woodcock CL, Hansen JC. Intrinsic disorder and autonomous domain function in the multifunctional nuclear protein, MeCP2. J Biol Chem 2007;282:15057–15064. [PubMed: 17371874]

Agarwal N, Hardt T, Brero A, Nowak D, Rothbauer U, Becker A, Leonhardt H, Cardoso MC. MeCP2 interacts with HP1 and modulates its heterochromatin association during myogenic differentiation. Nucleic Acids Res 2007;35:5402–5408. [PubMed: 17698499]

Ballestar E, Yusufzai TM, Wolffe AP. Effects of Rett syndrome mutations of the methyl-CpG binding domain of the transcriptional repressor MeCP2 on selectivity for association with methylated DNA. Biochemistry 2000;39:7100–7106. [PubMed: 10852707]

Brero A, Easwaran HP, Nowak D, Grunewald I, Cremer T, Leonhardt H, Cardoso MC. Methyl CpG-binding proteins induce large-scale chromatin reorganization during terminal differentiation. J Cell Biol 2005;169:733–743. [PubMed: 15939760]

Buschdorf JP, Stratling WH. A WW domain binding region in methyl-CpG-binding protein MeCP2: impact on Rett syndrome. J Mol Med 2004;82:135–143. [PubMed: 14618241]

Carro S, Bergo A, Mengoni M, Bachi A, Badaracco G, Kilstrup-Nielsen C, Landsberger N. A novel protein, Xenopus p20, influences the stability of MeCP2 through direct interaction. J Biol Chem 2004;279:25623–25631. [PubMed: 15056664]

Chadwick LH, Wade PA. MeCP2 in Rett syndrome: transcriptional repressor or chromatin architectural protein? Curr Opin Genet Dev 2007;17:121–125. [PubMed: 17317146]

Chandler SP, Guschin D, Landsberger N, Wolffe AP. The methyl-CpG binding transcriptional repressor MeCP2 stably associates with nucleosomal DNA. Biochemistry 1999;38:7008–7018. [PubMed: 10353812]

Chen WG, Chang Q, Lin Y, Meissner A, West AE, Griffith EC, Jaenisch R, Greenberg ME. Derepression of BDNF transcription involves calcium-dependent phosphorylation of MeCP2. Science 2003;302:885–889. [PubMed: 14593183]

Cheutin T, McNairn AJ, Jenuwein T, Gilbert DM, Singh PB, Misteli T. Maintenance of stable heterochromatin domains by dynamic HP1 binding. Science 2003;299:721–725. [PubMed: 12560555]

Dragich JM, Kim YH, Arnold AP, Schanen NC. Differential distribution of the MeCP2 splice variants in the postnatal mouse brain. J Comp Neurol 2007;501:526–542. [PubMed: 17278130]

Drewell RA, Goddard CJ, Thomas JO, Surani MA. Methylation-dependent silencing at the H19 imprinting control region by MeCP2. Nucleic Acids Res 2002;30:1139–1144. [PubMed: 11861904]

Festenstein R, Pagakis SN, Hiragami K, Lyon D, Verreault A, Sekkali B, Kioussis D. Modulation of heterochromatin protein 1 dynamics in primary Mammalian cells. Science 2003;299:719–721. [PubMed: 12560554]

Free A, Wakefield RI, Smith BO, Dryden DT, Barlow PN, Bird AP. DNA recognition by the methyl-CpG binding domain of MeCP2. J Biol Chem 2001;276:3353–3360. [PubMed: 11035019]

Fuks F, Hurd PJ, Wolf D, Nan X, Bird AP, Kouzarides T. The methyl-CpG-binding protein MeCP2 links DNA methylation to histone methylation. J Biol Chem 2003;278:4035–4040. [PubMed: 12427740]

Georgel PT, Horowitz-Scherer RA, Adkins N, Woodcock CL, Wade PA, Hansen JC. Chromatin compaction by human MeCP2. Assembly of novel secondary chromatin structures in the absence of DNA methylation. J Biol Chem 2003;278:32181–32188. [PubMed: 12788925]

Harikrishnan KN, Chow MZ, Baker EK, Pal S, Bassal S, Brasacchio D, Wang L, Craig JM, Jones PL, Sif S, et al. Brahma links the SWI/SNF chromatin-remodeling complex with MeCP2-dependent transcriptional silencing. Nat Genet 2005;37:254–264. [PubMed: 15696166]

Heitmann B, Maurer T, Weitzel JM, Stratling WH, Kalbitzer HR, Brunner E. Solution structure of the matrix attachment region-binding domain of chicken MeCP2. Eur J Biochem 2003;270:3263–3270. [PubMed: 12869202]

Horike S, Cai S, Miyano M, Cheng JF, Kohwi-Shigematsu T. Loss of silent-chromatin looping and impaired imprinting of DLX5 in Rett syndrome. Nat Genet 2005;37:31–40. [PubMed: 15608638]

Jones PL, Veenstra GJ, Wade PA, Vermaak D, Kass SU, Landsberger N, Strouboulis J, Wolffe AP. Methylated DNA and MeCP2 recruit histone deacetylase to repress transcription. Nat Genet 1998;19:187–191. [PubMed: 9620779]

Kimura H, Cook PR. Kinetics of core histones in living human cells: little exchange of H3 and H4 and some rapid exchange of H2B. J Cell Biol 2001;153:1341–1353. [PubMed: 11425866]

Kimura H, Shiota K. Methyl-CpG-binding protein, MeCP2, is a target molecule for maintenance DNA methyltransferase, Dnmt1. J Biol Chem 2003;278:4806–4812. [PubMed: 12473678]

Klose RJ, Bird AP. MeCP2 behaves as an elongated monomer that does not stably associate with the Sin3a chromatin remodeling complex. J Biol Chem 2004;279:46490–46496. [PubMed: 15322089]

Klose RJ, Sarraf SA, Schmiedeberg L, McDermott SM, Stancheva I, Bird AP. DNA binding selectivity of MeCP2 due to a requirement for A/T sequences adjacent to methyl-CpG. Mol Cell 2005;19:667–678. [PubMed: 16137622]

Koch C, Stratling WH. DNA binding of methyl-CpG-binding protein MeCP2 in human MCF7 cells. Biochemistry 2004;43:5011–5021. [PubMed: 15109260]

Kokura K, Kaul SC, Wadhwa R, Nomura T, Khan MM, Shinagawa T, Yasukawa T, Colmenares C, Ishii S. The Ski protein family is required for MeCP2-mediated transcriptional repression. J Biol Chem 2001;276:34115–34121. [PubMed: 11441023]

Kriaucionis S, Bird A. The major form of MeCP2 has a novel N-terminus generated by alternative splicing. Nucleic Acids Res 2004;32:1818–1823. [PubMed: 15034150]

Kudo S, Nomura Y, Segawa M, Fujita N, Nakao M, Dragich J, Schanen C, Tamura M. Functional analyses of MeCP2 mutations associated with Rett syndrome using transient expression systems. Brain Dev 2001;23(Suppl 1):S165–S173. [PubMed: 11738866]

Kudo S, Nomura Y, Segawa M, Fujita N, Nakao M, Schanen C, Tamura M. Heterogeneity in residual function of MeCP2 carrying missense mutations in the methyl CpG binding domain. J Med Genet 2003;40:487–493. [PubMed: 12843318]

Leonard H, Colvin L, Christodoulou J, Schiavello T, Williamson S, Davis M, Ravine D, Fyfe S, de Klerk N, Matsuishi T, et al. Patients with the R133C mutation: is their phenotype different from patients with Rett syndrome with other mutations? J Med Genet 2003;40:e52. [PubMed: 12746406]

Lever MA, Th'ng JP, Sun X, Hendzel MJ. Rapid exchange of histone H1.1 on chromatin in living human cells. Nature 2000;408:873–876. [PubMed: 11130728]

Marchi M, Guarda A, Bergo A, Landsberger N, Kilstrup-Nielsen C, Ratto GM, Costa M. Spatio-temporal dynamics and localization of MeCP2 and pathological mutants in living cells. Epigenetics 2007;2:187–197. [PubMed: 17965612]

Martinowich K, Hattori D, Wu H, Fouse S, He F, Hu Y, Fan G, Sun YE. DNA methylation-related chromatin remodeling in activity-dependent BDNF gene regulation. Science 2003;302:890–893. [PubMed: 14593184]

Meehan RR, Lewis JD, Bird AP. Characterization of MeCP2, a vertebrate DNA binding protein with affinity for methylated DNA. Nucleic Acids Res 1992;20:5085–5092. [PubMed: 1408825]

Misteli T, Gunjan A, Hock R, Bustin M, Brown DT. Dynamic binding of histone H1 to chromatin in living cells. Nature 2000;408:877–881. [PubMed: 11130729]

Miyake K, Nagai K. Phosphorylation of methyl-CpG binding protein 2 (MeCP2) regulates the intracellular localization during neuronal cell differentiation. Neurochem Int 2007;50:264–270. [PubMed: 17052801]

Mnatzakanian GN, Lohi H, Munteanu I, Alfred SE, Yamada T, MacLeod PJ, Jones JR, Scherer SW, Schanen NC, Friez MJ, et al. A previously unidentified MECP2 open reading frame defines a new protein isoform relevant to Rett syndrome. Nat Genet 2004;36:339–341. [PubMed: 15034579]

Nan X, Meehan RR, Bird A. Dissection of the methyl-CpG binding domain from the chromosomal protein MeCP2. Nucleic Acids Res 1993;21:4886–4892. [PubMed: 8177735]

Nan X, Tate P, Li E, Bird A. DNA methylation specifies chromosomal localization of MeCP2. Mol Cell Biol 1996;16:414–421. [PubMed: 8524323]

Nan X, Campoy FJ, Bird A. MeCP2 is a transcriptional repressor with abundant binding sites in genomic chromatin. Cell 1997;88:471–481. [PubMed: 9038338]

Nan X, Ng HH, Johnson CA, Laherty CD, Turner BM, Eisenman RN, Bird A. Transcriptional repression by the methyl-CpG-binding protein MeCP2 involves a histone deacetylase complex. Nature 1998;393:386–389. [PubMed: 9620804]

Nan X, Hou J, Maclean A, Nasir J, Lafuente MJ, Shu X, Kriaucionis S, Bird A. Interaction between chromatin proteins MECP2 and ATRX is disrupted by mutations that cause inherited mental retardation. Proc Natl Acad Sci USA 2007;104:2709–2714. [PubMed: 17296936]

Nikitina T, Shi X, Ghosh RP, Horowitz-Scherer RA, Hansen JC, Woodcock CL. Multiple modes of interaction between the methylated DNA binding protein MeCP2 and chromatin. Mol Cell Biol 2007;27:864–877. [PubMed: 17101771]

Ohki I, Shimotake N, Fujita N, Nakao M, Shirakawa M. Solution structure of the methyl-CpG-binding domain of the methylation-dependent transcriptional repressor MBD1. EMBO J 1999;18:6653–6661. [PubMed: 10581239]

Ohki I, Shimotake N, Fujita N, Jee J, Ikegami T, Nakao M, Shirakawa M. Solution structure of the methyl-CpG binding domain of human MBD1 in complex with methylated DNA. Cell 2001;105:487–497. [PubMed: 11371345]

Phair RD, Misteli T. High mobility of proteins in the mammalian cell nucleus. Nature 2000;404:604–609. [PubMed: 10766243]

Richard-Foy H, Hager GL. Sequence-specific positioning of nucleosomes over the steroid-inducible MMTV promoter. EMBO J 1987;6:2321–2328. [PubMed: 2822386]

Shahbazian MD, Zoghbi HY. Molecular genetics of Rett syndrome and clinical spectrum of MECP2 mutations. Curr Opin Neurol 2001;14:171–176. [PubMed: 11262731]

Shahbazian MD, Zoghbi HY. Rett syndrome and MeCP2: linking epigenetics and neuronal function. Am J Hum Genet 2002;71:1259–1272. [PubMed: 12442230]

Smeets E, Terhal P, Casaer P, Peters A, Midro A, Schollen E, van Roozendaal K, Moog U, Matthijs G, Herbergs J, et al. Rett syndrome in females with CTS hot spot deletions: a disorder profile. Am J Med Genet A 2005;132:117–120. [PubMed: 15578576]

Stancheva I, Collins AL, Van den Veyver IB, Zoghbi H, Meehan RR. A mutant form of MeCP2 protein associated with human Rett syndrome cannot be displaced from methylated DNA by notch in Xenopus embryos. Mol Cell 2003;12:425–435. [PubMed: 14536082]

Suzuki M, Yamada T, Kihara-Negishi F, Sakurai T, Oikawa T. Direct association between PU. 1 and MeCP2 that recruits mSin3A-HDAC complex for PU.1-mediated transcriptional repression. Oncogene 2003;22:8688–8698. [PubMed: 14647463]

Thatcher KN, Peddada S, Yasui DH, Lasalle JM. Homologous pairing of 15q11-13 imprinted domains in brain is developmentally regulated but deficient in Rett and autism samples. Hum Mol Genet 2005;14:785–797. [PubMed: 15689352]

Tudor M, Akbarian S, Chen RZ, Jaenisch R. Transcriptional profiling of a mouse model for Rett syndrome reveals subtle transcriptional changes in the brain. Proc Natl Acad Sci USA 2002;99:15536–15541. [PubMed: 12432090]

Wade PA. Methyl CpG-binding proteins and transcriptional repression. BioEssays 2001;23:1131–1137. [PubMed: 11746232]

Wakefield RI, Smith BO, Nan X, Free A, Soteriou A, Uhrin D, Bird AP, Barlow PN. The solution structure of the domain from MeCP2 that binds to methylated DNA. J Mol Biol 1999;291:1055–1065. [PubMed: 10518942]

Yasui DH, Peddada S, Bieda MC, Vallero RO, Hogart A, Nagarajan RP, Thatcher KN, Farnham PJ, Lasalle JM. Integrated epigenomic analyses of neuronal MeCP2 reveal a role for long-range interaction with active genes. Proc Natl Acad Sci USA 2007;104:19416–19421. [PubMed: 18042715]

Young JI, Hong EP, Castle JC, Crespo-Barreto J, Bowman AB, Rose MF, Kang D, Richman R, Johnson JM, Berget S, et al. Regulation of RNA splicing by the methylation-dependent transcriptional repressor methyl-CpG binding protein 2. Proc Natl Acad Sci USA 2005;102:17551–17558. [PubMed: 16251272]

Yusufzai TM, Wolffe AP. Functional consequences of Rett syndrome mutations on human MeCP2. Nucleic Acids Res 2000;28:4172–4179. [PubMed: 11058114]

Zhou Z, Hong EJ, Cohen S, Zhao WN, Ho HY, Schmidt L, Chen WG, Lin Y, Savner E, Griffith EC, et al. Brain-specific phosphorylation of MeCP2 regulates activity-dependent Bdnf transcription, dendritic growth, and spine maturation. Neuron 2006;52:255–269. [PubMed: 17046689]

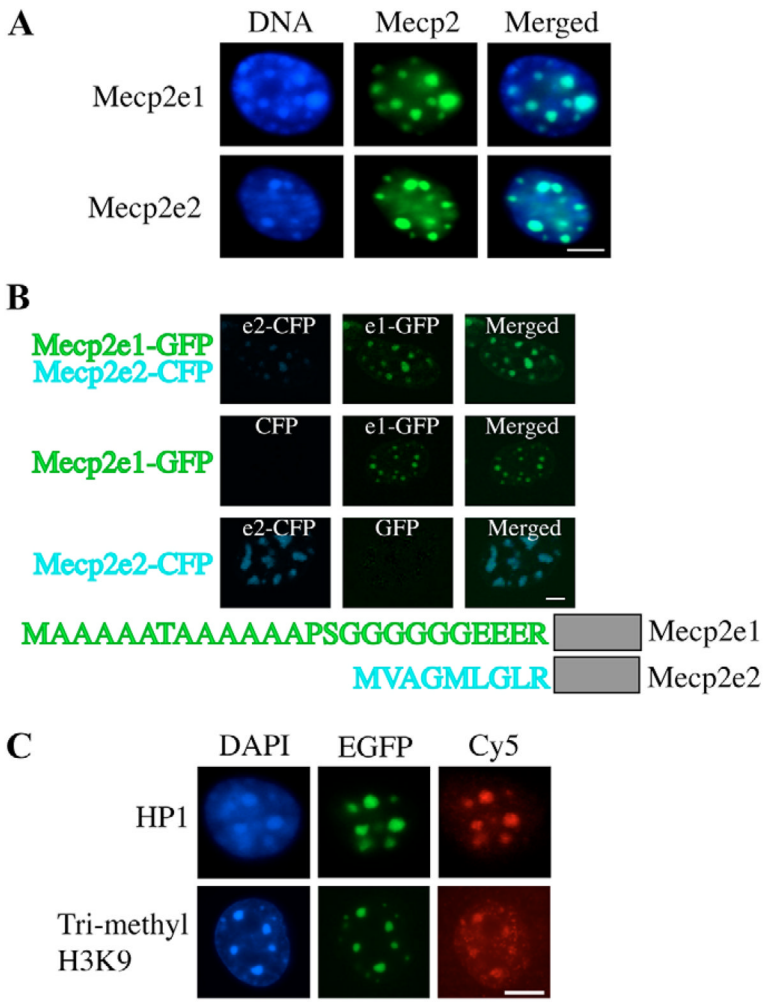

Fig. 1.

MECP2e1 and MECP2e2 colocalize in pericentromeric heterochromatin along with other heterochromatin marker proteins. (A) Balb/c 3T3 cells expressing EGFP-tagged MECP2e1 and MECP2e2 were stained with the DNA stain DAPI and imaged by epifluorescence microscopy. Bar, 5 μm. (B) Balb/c 3T3 cells were co-transfected with MECP2e2 tagged with ECFP and MECP2e1 tagged with EGFP. Cells were induced with 100 μM Zn^{2+} and imaged by confocal microscopy applying the online fingerprinting mode to separate the overlapping spectra. Bar, 1 μm. (C) Cells expressing EGFP-tagged MECP2e2 were immunostained with heterochromatin protein 1 (HP1) and histone H3 trimethylated at lysine 9. Bar, 5 μm.

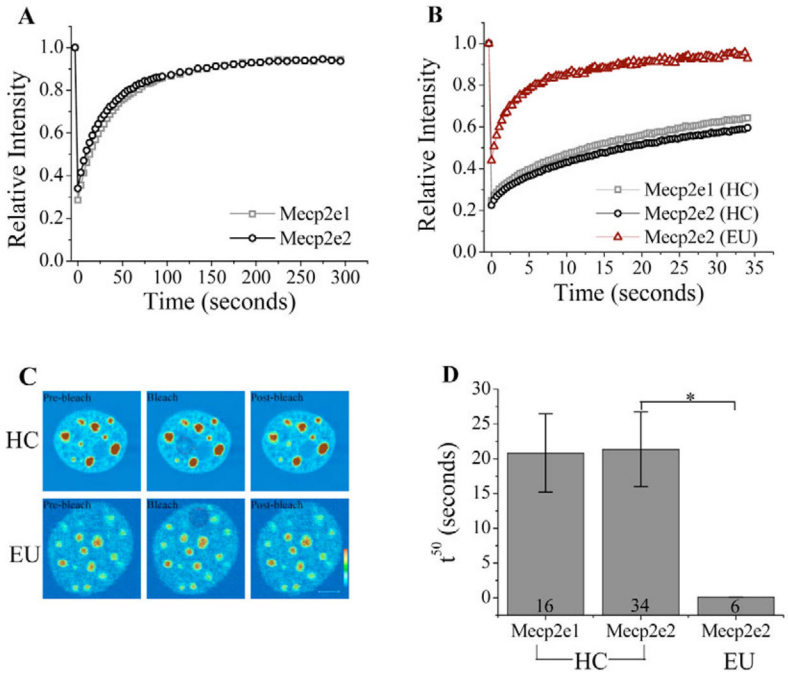

Fig. 2.

MECP2e1 and MECP2e2 are mobile in vivo and demonstrate identical kinetics. (A) FRAP was performed on EGFP-tagged MECP2e1 and MECP2e2. Individual pericentromeric heterochromatin foci were photobleached and the recovery was monitored over time. The intensity in the photobleached region was normalized to total nuclear intensity and plotted as a function of time. The recovery curves indicate rapid binding kinetics of both protein isoforms and nearly complete recovery of fluorescence within the bleached area. (B) Early recovery kinetics for the two protein isoforms were examined by performing FRAP experiments at a high scan speed of 323 mseconds. The rapid recovery kinetics of MECP2e2 in euchromatin are also shown. HC, heterochromatin; EU, euchromatin. (C) The upper panels demonstrate a bleaching sequence of a heterochromatic focus in a MECP2e2-expressing cell. The lower panels show a similar sequence in a euchromatic area of the nucleus. Bar, 5 μm. (D) The t^{50} values were determined by fitting the recovery curves. The t^{50} values of the two isoforms in heterochromatin are not statistically significant (MECP2e1=20.8±5.6 and MECP2e2=21.3 ±5.4). By contrast, the mobility of MECP2e2 in euchromatin is extremely rapid (t^{50}=0.125 ±0.003; **P*<0.0001). The number of nuclei photobleached is shown within each bar.

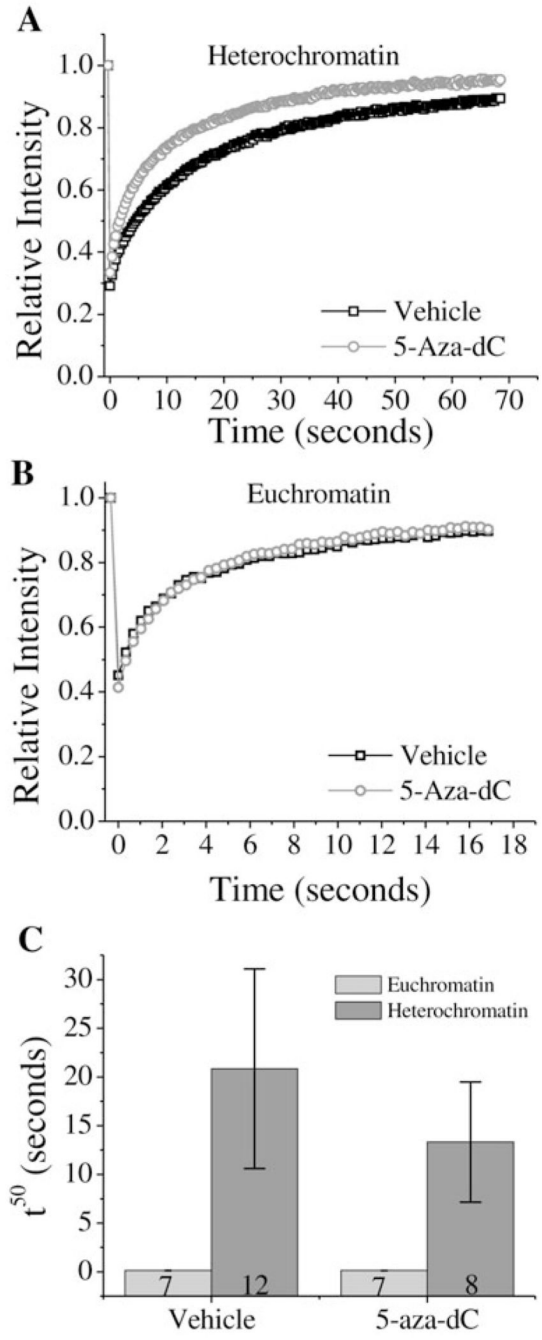

Fig. 3.

Treatment with the DNA demethylating agent 5-Aza-2-deoxycytidine does not significantly alter MECP2e2 dynamics. (A) Balb/c 3T3 cells were treated with 1 μM 5-Aza-2-deoxycytidine (5-Aza-dC) for 5 days then transiently transfected with the human MECP2e2-GFP construct driven by the CMV promoter. 48 hours post-transfection, cells were photobleached. The recovery profiles of 5-Aza-dC-treated and untreated cells in heterochromatic regions are shown. The slight leftwards shift in the recovery curve was noted. (B) Recovery kinetics of 5-aza-dC treated and vehicle (DMSO) control in euchromatic regions are shown and indicate no changes in mobility associated with drug treatment. (C) Although there was a slight shift in the recovery curve in heterochromatin, the differences in the t^{50} values following 5-Aza-dC

treatment were not statistically significant in either heterochromatin and euchromatin. The t^{50} values of vehicle and 5-Aza-dC treated cells in heterochromatin are 20.9±10.2 and 13.3 ±6.1, respectively (P=0.0798). In euchromatin, the t^{50} values of vehicle and 5-Aza-dC-treated cells are 0.13±0.01 and 0.13±0.008, respectively (P=0.7561). The number of nuclei photobleached in each group is shown within the bar.

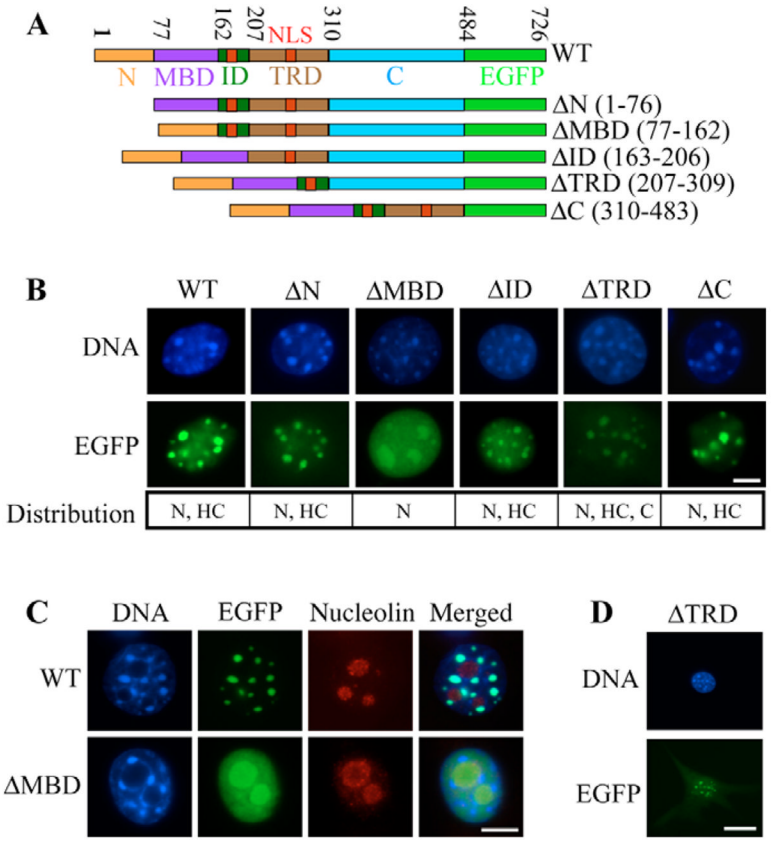

Fig. 4.

Expression constructs of MECP2 and their cellular localization. (A) Schematic showing the expression constructs of MECP2 that were used in the domain-deletion studies. Deleted residues based on murine MECP2e2 are shown in parentheses. The locations of NLS are shown as red boxes. (B) Cells expressing EGFP-tagged WT and mutant proteins were stained with DAPI and imaged by epifluorescence microscopy. The cellular distribution of the proteins is indicated (N, nuclear; HC, heterochromatin; C, cytoplasmic). (C) Deletion of the MBD results in the mislocalization of MECP2 to the nucleolus. Stable cell lines expressing EGFP-tagged WT and ΔMBD were immunostained with the nucleolar marker nucleolin and counterstained with DAPI. (D) Cells expressing the ΔTRD mutant showing both cytoplasmic and nuclear localization. Bars, 5 μm.

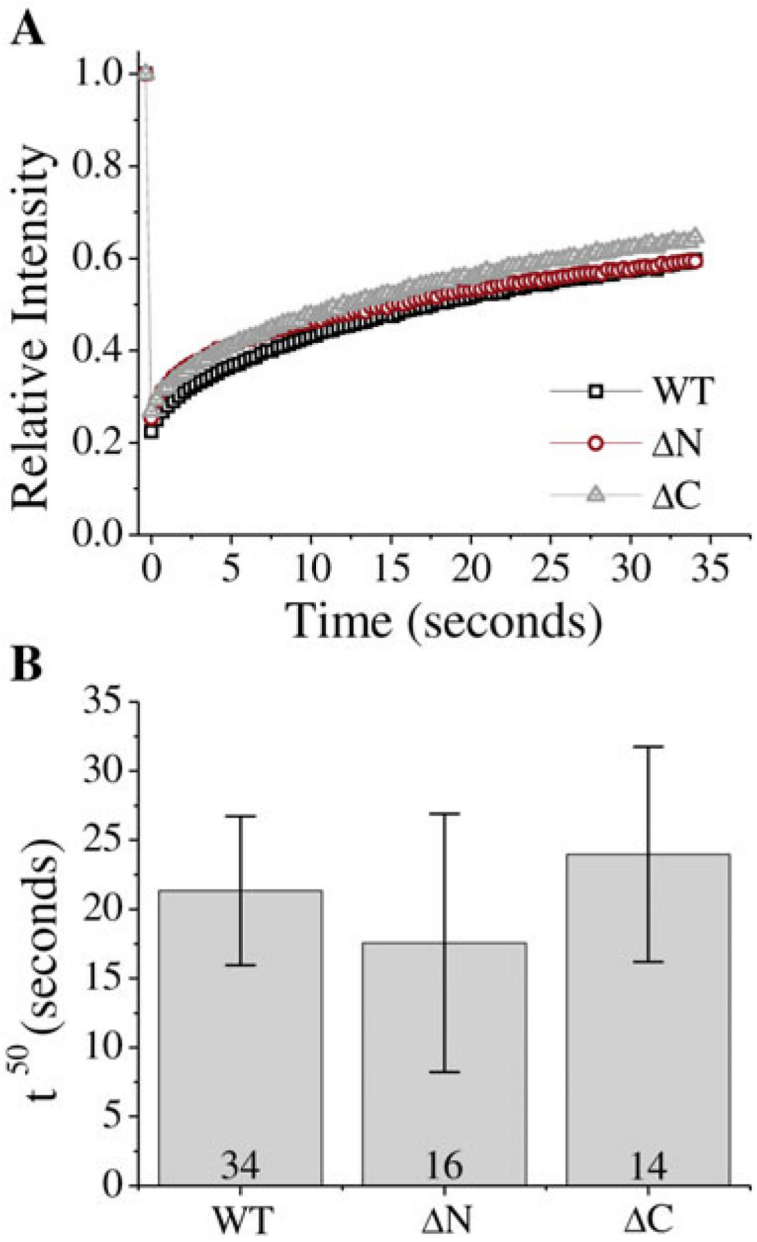

Fig. 5.

Deletion of the N- or C-terminus of MECP2 does not have any significant impact on its mobility. (A) Cells expressing EGFP-tagged MECP2e2 (WT), ΔN and ΔC were photobleached and their recovery curves were plotted, revealing essentially no differences in binding kinetics for the deleted proteins. (B) Curve fitting was used to determine t^{50} values±s.d. for each of the protein forms (21.3±5.4, 17.6±9.3 and 23.9±7.8 for WT, ΔN and ΔC, respectively). The t^{50} values of ΔN and ΔC are not significantly different from WT (P>0.05). The number of nuclei photobleached in each group is shown within the bars.

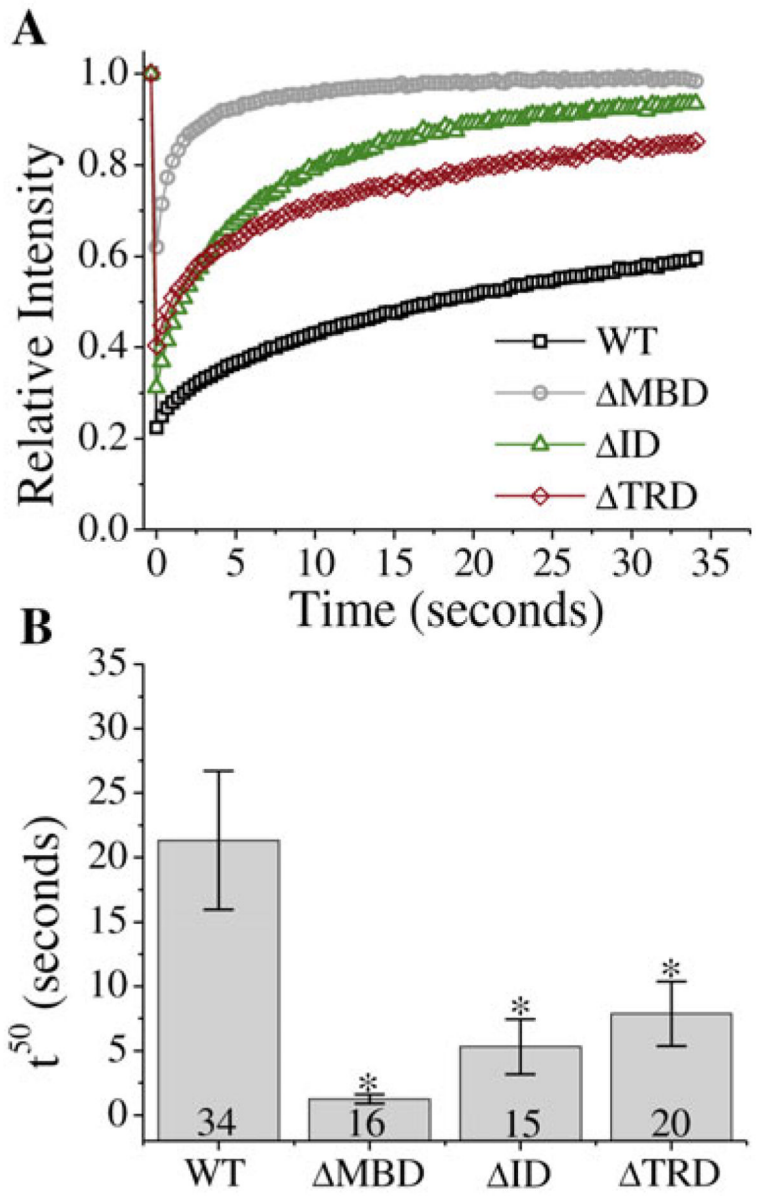

Fig. 6.

Deletion of the MBD, interdomain region and the TRD impact mobility of MECP2. (A) Recovery kinetics of the domain-deleted mutant forms indicate that that the MBD, ID and TRD contribute to the mobility. (B) The t^{50} values for the domain-deleted proteins indicate increased mobility for the protein within heterochromatin domains for the ΔID and ΔTRD proteins compared with WT. The t^{50} for the ΔMBD in nucleoplasm was intermediate between the value for euchromatin and heterochromatin for the WT protein (WT=21.3±5.4, ΔMBD=1.3±0.4, ΔID=5.3±2.1 and ΔTRD=7.9±2.5). Asterisks represent t^{50} values that are significantly different from heterochromatin in WT (P<0.0001). Number of nuclei for each group is shown within each bar.

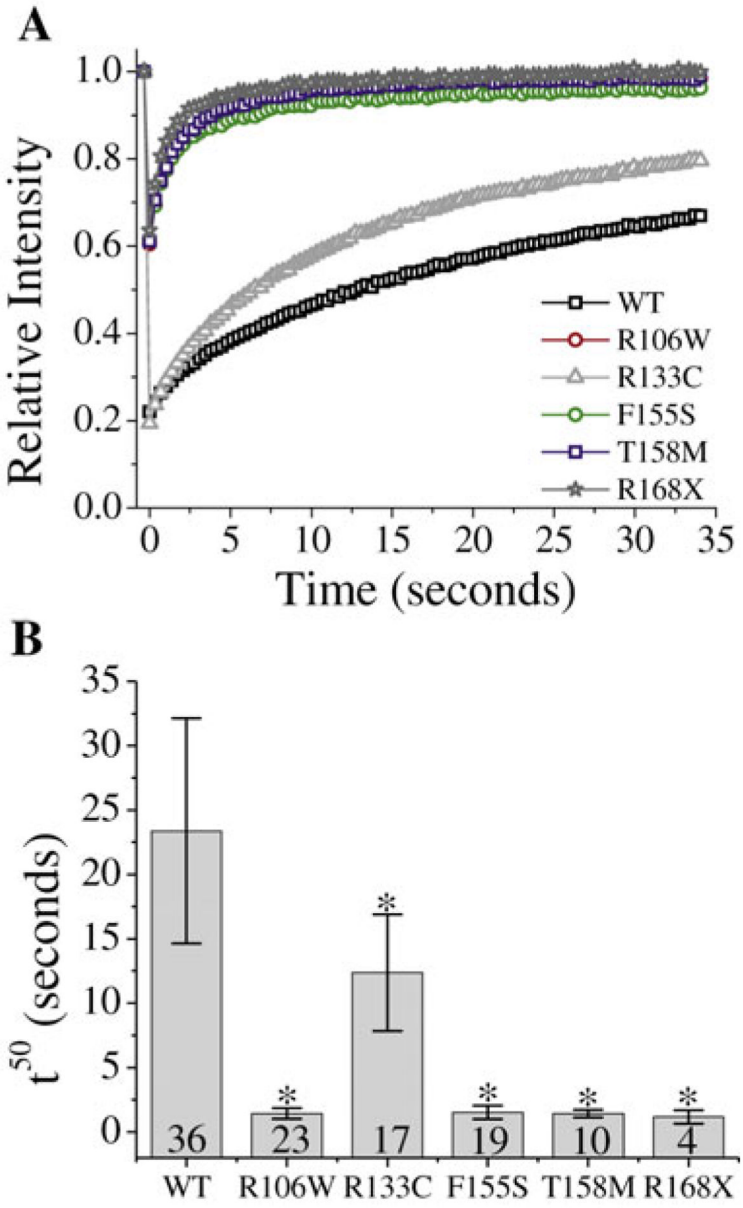

Fig. 7.

Common RTT mutations significantly impact mobility of MECP2. (A) Recovery profiles of MECP2e2 (WT) and common RTT mutations of MECP2 found in the patient population. Balbc/3T3 cells were transiently transfected with CMV driven expression constructs encoding N-terminus EGFP-tagged MECP2, including common RTT mutations. Photobleaching was performed in regions of nucleoplasm (R106W, F155S, T158M) or heterochromatin (R133C, R168X). (B) The t^{50} values of the WT and RTT mutants (WT=23.4±8.8, R106W=1.4±0.42, R133C=12.4±4.5, F155S=1.5±0.5, T158M=1.4±0.3 and R168X=1.17±0.5). The sample size for each group is given within the bars. Asterisks represent significant different values compared with the WT protein in heterochromatin (P<0.0001).

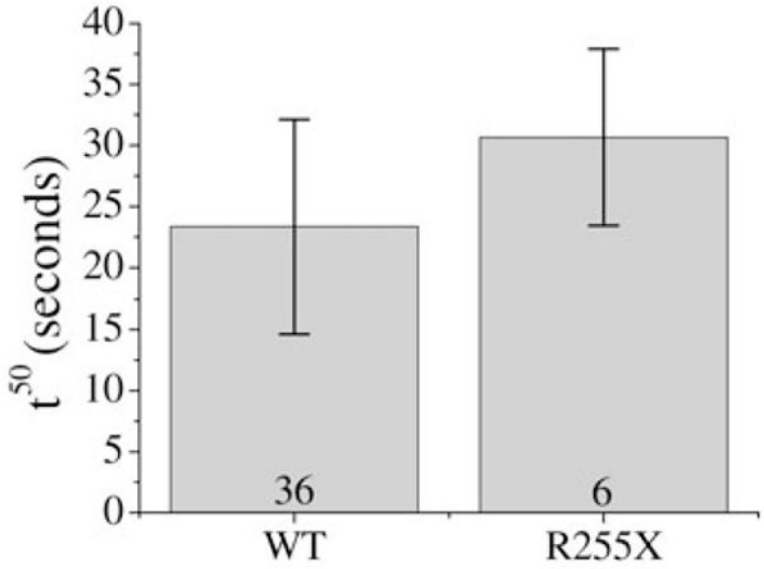

Fig. 8.

The t^{50} value of R255X does not differ significantly from WT protein. The binding kinetics for the R255X mutant protein are not significantly different than WT. A two-tailed *t*-test does not reveal a statistically significant difference in the t^{50} values between the two groups (*P*=0.0608). The number of nuclei is shown within each bar.

Table 1

Summary of binding kinetics

Construct	Photobleached region	t^{50} ± s.d. (seconds)	t^{90} ± s.d. (seconds)
Mecp2e1	HC	20.8±5.6	168.8±18.4
WT mouse	HC	21.3±5.4	169.0±21.8
WT mouse	EU	0.13±0.003	1.13±0.03
ΔN	HC	17.6±9.3	143.6±21.6
ΔMBD	NP	1.3±0.4	11.3±3.3
ΔID	HC	5.3±2.1	37.2±8.7
ΔTRD	HC	7.9±2.5	77.5±11.6
ΔC	HC	23.9±7.8	163.5±23.4
WT human	HC	23.4±8.8	156.2±22.0
R106W	NP	1.4±0.42	12.3±3.2
R133C	HC	12.4±4.5	84.0±10.4
F155S	NP	1.5±0.5	13.7±4.7
T158M	NP	1.4±0.3	12.8±2.7
R168X	HC	1.2±0.5	8.4±2.7

t^{50} and t^{90} values of domain deletion and RTT mutants. HC, heterochromatin; EU, euchromatin; NP, nucleoplasm.